

An Analytical Model for CBAP Allocations in IEEE 802.11ad

Chiara Pielli, Tanguy Ropitault,
Nada Golmie, *Senior Member, IEEE*, and Michele Zorzi, *Fellow, IEEE*

Abstract—The IEEE 802.11ad standard extends WiFi operation to the millimeter wave frequencies, and introduces novel features concerning both the physical (PHY) and Medium Access Control (MAC) layers. The hybrid MAC layer provides for two different kinds of resource allocations: Contention Based Access Periods (CBAPs) and contention-free Service Periods (SPs). In this paper, we propose a Markov Chain model to represent CBAPs, taking into account operation interruptions due to scheduled SPs and the deafness and hidden node problems that directional communication exacerbates. We also propose a mathematical analysis to evaluate the interference among stations and derive analytical expressions to assess the impact of various system parameters on some key performance metrics such as throughput, delay, and packet drop rate. This information may be used to efficiently design a transmission scheduler that allocates contention-based and contention-free periods based on the application requirements.

I. INTRODUCTION

The IEEE 802.11ad standard [1] is designed to operate in the 60 GHz ISM unlicensed band and targets short range millimeter wave (mmWave) communications in Local Area Networks (LANs). MmWaves have been gaining a lot of momentum in telecommunications, because the wide spectrum available at such frequencies enables channels with higher capacity, which have the potential to eliminate the congestion issues of the overcrowded sub-6-GHz bands. However, the propagation environment in the mmWave spectrum is significantly different from that at sub-6-GHz frequencies, and is characterized by severe propagation loss and sensitivity to blockage, i.e., high attenuation due to obstacles. The beamforming technique, which consists in focusing all the power towards a specific direction, allows to increase the coverage range, and also attenuates the interference among concurrent transmissions.

Because of the peculiar characteristics of the mmWave propagation environment, protocols designed for lower frequencies cannot simply be transposed to the mmWave band, but major design changes are required for both PHY and Medium Access Control (MAC) layers. While extensive research is ongoing to develop efficient beamforming training and beam tracking

Chiara Pielli (piellich@dei.unipd.it) and Michele Zorzi (zorzi@dei.unipd.it) are with the Department of Information Engineering, University of Padova, Padova, Italy. Tanguy Ropitault (tanguy.ropitault@nist.gov) and Nada Golmie (nada.golmie@nist.gov) are with the National Institute of Standards and Technology (NIST), Gaithersburg, MD, US.

The identification of any commercial product or trade name does not imply endorsement or recommendation by the National Institute of Standards and Technology, nor is it intended to imply that the materials or equipment identified are necessarily the best available for the purpose.

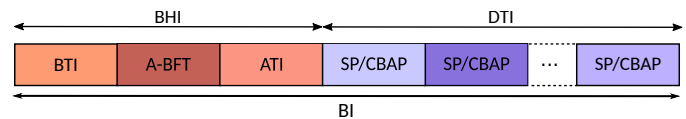


Figure 1: Structure of a BI. Its maximum allowed duration is 1 s.

mechanisms to establish and maintain directional links [2], [3], it is also necessary to understand *how* to access the wireless medium and use the beamformed links efficiently to transmit data. The MAC layer of 802.11ad provides for both contention-based and contention-free allocations, plus an additional mechanism built on top of the predefined schedule to dynamically allocate the channel in quasi real-time. In our vision, the potentially outstanding flexibility of 802.11ad can be unleashed through an adaptive scheduler that selects the most appropriate allocation based on the traffic characteristics. However, the standard [1] only provides rules for channel access, and, to the best of our knowledge, efficient scheduling schemes that exploit this hybrid MAC layer are yet to be developed.

In this paper, we focus on the performance that can be obtained in Contention Based Access Period (CBAP) allocations, taking into account the presence of the contention-free Service Period (SP) allocations. This is intended to represent a first step in the characterization of the allocations available in 802.11ad, with the ultimate goal of designing an efficient allocation scheduler able to cope with heterogeneous traffic patterns and requirements. In particular, we propose a variation of Bianchi’s seminal model for the Distributed Coordination Function (DCF) mechanism in legacy WiFi networks [4]. Such variation addresses the main novel features of 802.11ad and, unlike most of the works proposed in the literature, takes into account the deafness and hidden node problems, which are exacerbated by directional transmissions [5].

The rest of the paper is structured as follows. Sec. II gives an overview of the data transmission mechanisms in 802.11ad, while Sec. III introduces the related works. The proposed model and the metrics used to evaluate the performance are described in Secs. IV and V, respectively. Sec. VI explains how to compute the interference regions when constant-gain beam shapes are used. Sec. VII shows the numerical evaluations and, finally, Sec. VIII concludes the paper.

II. DATA TRANSMISSION IN 802.11AD

The medium access time is divided into Beacon Intervals (BIs), each composed of a Beacon Header Interval (BHI) and a Data Transmission Interval (DTI), as shown in Fig. 1.

The BHI is used for synchronization, network management, and beamforming training between the STAs and the PCP/AP¹. It includes up to three access periods, all of them optional: the Beacon Transmission Interval (BTI), the Association-Beamforming Training (A-BFT), and the Announcement Transmission Interval (ATI).

The DTI is used for data transmission and for beamforming training with the PCP/AP and between STAs. It is made up of two very different schemes, namely, contention-free SPs for exclusive communication between dedicated pairs of STAs, and CBAPs where STAs compete for access. SPs and CBAPs can be in any number and combination, and their schedule is advertised by the PCP/AP in the BTI and/or in the ATI [1]. Note that this schedule is set up prior to the beginning of the DTI. In addition, a dynamic channel time allocation mechanism allows STAs to reserve channel time in almost real-time over both SPs and CBAPs, as STAs can be polled by the PCP/AP and ask for channel time, which will be granted back to back.

A. Contention-based access

CBAPs follow the Enhanced Distributed Channel Access (EDCA) mechanism, which is an enhanced DCF that includes frame aggregation, block acknowledgments and functionalities to handle traffic categories. STAs compete for access and can obtain Transmission Opportunities (TXOPs) (contention-free periods) by winning an instance of EDCA contention. The DCF and the EDCA are based on Carrier Sense Multiple Access with Collision Avoidance (CSMA/CA): before transmission, the channel has to be sensed idle for a minimum amount of time, namely a Distributed Interframe Space (DIFS). If the channel is sensed busy, the transmission is postponed: the station (STA) picks a backoff counter uniformly distributed in $\{0, \dots, W_i - 1\}$, where W_i is the size of the contention window at the i -th retransmission attempt. The contention window doubles at each collision ($W_i = 2^i W_0$), until it saturates to a maximum value. The backoff counter is decremented as long as the channel is sensed idle, frozen when the channel is sensed busy or the CBAP operation is suspended (because the DTI ends or due to the presence of an SP), and reactivated when the channel is sensed idle again for at least a DIFS (after the CBAP operation has been resumed). When the backoff counter expires, the STA accesses the channel.

In 802.11ad, the channel status is determined through a combined physical and virtual carrier sensing; the former consists in energy or preamble detection over the channel, the latter is realized through Network Allocation Vectors (NAVs). The NAVs are counters based on the information announced in Request-To-Send (RTS) and Clear-To-Send (CTS) frames prior to the actual exchange of data and maintain a prediction of future traffic on the medium. The directional nature of communication at mmWaves makes the carrier sensing operations problematic because there may be interference even though

¹Besides the traditional WiFi network topology, 802.11ad can also be used for Personal Basic Service Sets (PBSSs), i.e., network architectures for ad hoc modes. The central coordinator of 802.11ad networks can then be either a PBSS Control Point (PCP) or an Access Point (AP); accordingly, it is generally denoted as PCP/AP to include both infrastructures.

the medium was sensed to be idle [6]. Note that 802.11ad introduces the concept of antenna sectors, which correspond to a discretization of the antenna space and reduce the number of possible beam directions to try in the beamforming.

III. RELATED WORK

The seminal work of Bianchi [4] introduces a Markov Chain (MC) model of the 802.11 DCF. Although several variations of such model have been proposed to account for, e.g., a finite number of retransmissions [7], a heterogeneous Quality of Service (QoS) [8] and the hidden node problem [9], none of them can be readily applied to the hybrid MAC layer of 802.11ad, as different changes are needed to account for its peculiar features.

Some works in the literature propose adaptations of Bianchi's model for 802.11ad. For example, [10] uses a 3-dimensional MC to analyze the channel utilization and the average MAC layer delay in CBAPs, [11] models CBAPs with a 2-dimensional MC for unsaturated sources considering also the presence of SPs, and also [12] uses a 2-dimensional MC to analyze the saturation throughput in CBAPs.

However, such works do not accurately model the effect of directional communication. In our opinion, the following are the most common assumptions that may alter the validity of the performance analyses. First (see [10], [11], [12]), the area around the PCP/AP is divided into sectors which are served in a round-robin fashion, i.e., CBAPs are allocated to a single sector at a time, so that two STAs belonging to different sectors cannot compete for the channel time in the same allocation. This strongly affects the analysis of the delay and the impact of the number of sectors of the PCP/AP on the system performance. Notice that, according to the standard [1], this is not necessarily true, since any subset of stations can participate in a CBAP, with potential deafness and hidden node issues. The second common strong assumption (see [10], [11], [12], [13]) is that STAs listen to the channel and send RTS/CTS frames in quasi-omnidirectional (QO) mode, and all STAs in the same sector are aware of all the messages exchanged by the other nodes with the AP. This assumption is not very realistic, because transmissions over beamtrained links should be made directionally to avoid serious inefficiencies and short coverage range. Third (see [11], [12]), the DTI is assumed to be made of SP allocations followed by a single CBAP allocation at the end of the DTI, while the standard states that SPs and CBAPs can be in any number and order. This may strongly affect the delay, as different configurations of the DTI may yield different performance. Finally, [11] envisages a variable BI duration, depending on the number of SP and CBAP allocations: such condition is troublesome to achieve in practice, because a change in the BI duration has to be communicated to all the STAs in the network beforehand, and requires the PCP/AP to start spreading this information a predefined number of BIs prior to the activation of the change [1]. In our work, we do not make such assumptions, but rather consider that all the STAs contend for channel access in an allocation, and may collide due to deafness or hidden node problems.

A more accurate approach to directional communication in WiFi networks is presented in [14], which considers a

rigorous model for directional transmission, with the presence of side lobes with small antenna gain and corresponding regions with different levels of interference. However, the model is not designed for 802.11ad as it does not consider the presence of SP allocations and the related backoff counter freezing. Also [13] takes into account deafness and hidden node problems, and subdivides the area around a STA based on the interference level; CBAPs are then modeled using a 3-dimensional MC. Similarly, our model is based on a division of the area around a considered STA into regions: the other STAs can be grouped based on whether they can detect the uplink and/or downlink messages between the STA and the AP, according to their respective positions and beams. Differently from our work in this paper, [13] considers cooperation among STAs, with the possibility of using other STAs as relays for transmissions to the AP; we instead focus on a pure traditional WiFi topology, with the STAs able to communicate directly only with the AP. Due to this assumption, STAs in [13] listen to the channel in a QO mode if not already participating in a communication; on the other hand, in our scenario, STAs always have their trained receiving antennas directed towards the AP, so as to avoid the useless energy and time overhead of continuously switching antenna pattern. This difference results into two different ways of calculating the coverage regions of a STA.

Other works in the literature consider different aspects of the DTI. For example, [15] derives the theoretical maximum throughput for CBAPs when two-level MAC frame aggregation is used. [5] proposes a directional MAC protocol to be used on top of 802.11ad: it allows the use of sequential directional RTS messages that a STA sends in all directions. The beamforming issue is considered in [16], which proposes a joint optimization of beamwidth selection and scheduling to maximize the effective network throughput, while the problem of high collision probability and low beamforming training efficiency in dense 802.11ad scenarios is addressed in [17], where two mechanisms are proposed to reduce the collision probability in the A-BFT phase.

For what concerns SPs, an accurate mathematical model for their preliminary allocation is presented in [18]. It considers the presence of quasi-periodic structures with multiple blocks within the same allocation, the erroneous nature of the wireless medium, and the possibility of multiple consecutive transmissions within the same allocation.

IV. SYSTEM MODEL

We now introduce our analytical model for CBAP operation in 802.11ad. We denote as T_{BI} the duration of a BI and as T_{BHI} , T_{CBAP} and T_{SP} the time dedicated to BHI, CBAPs and SPs during a BI, respectively. The total time T_{CBAP} dedicated for contention-based access in a BI is distributed among N_{CBAP} allocations, while T_{SP} is distributed among N_{SP} allocations.

We only focus on the classic WiFi network where a certain number of STAs communicate solely with the AP and consider that the RTS/CTS mechanism is used. We make the following assumptions: i) all STAs in the network implement only a single traffic category, hence service differentiation is not

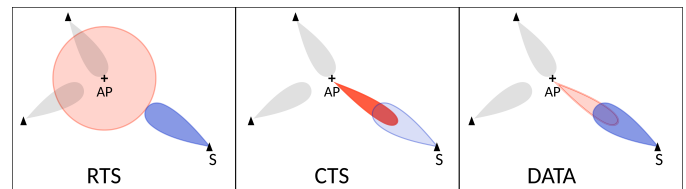


Figure 2: Communication phases between the AP and a target STA S , with 2 other STAs listening towards the AP. Darker beams indicate a transmission, while lighter ones that the device is listening. S directionally transmits the RTS while the AP is listening in QO mode; then the AP steers its antennas towards S and sends the CTS to S , that replies with a data message.

considered; ii) the beamforming training has already been performed, so that the STAs already know how to steer their antennas to communicate with the AP; and iii) we consider packet saturation at the MAC queue of each STA, implying that every STA has a head-of-line packet ready to join the contention process after the current packet is transmitted.

To assess the performance achievable in a CBAP, we leverage on Bianchi's seminal work [4] and adapt it to model the features of CBAPs in 802.11ad. First, we explain how directionality affects the communication during the contention-based channel access, then we describe the proposed model, and finally we discuss the performance metrics used in the numerical evaluation.

A. Directional communication in CBAPs

CBAPs are based on the EDCA, but the traditional approaches used in the literature need to be adapted to take directionality into account.

The most widely used approach in the literature to model the DCF and EDCA mechanisms is Bianchi's model [4]. It takes the perspective of a target node and models the backoff process as a 2-dimensional MC, where state (i, k) refers to the i^{th} backoff stage with the backoff counter $k \in \{0, \dots, W_i - 1\}$, where W_i is the duration of the contention window at the i^{th} retransmission attempt. The counter is decremented with probability 1 whenever the channel is sensed idle, and when it reaches 0 the STA attempts to transmit. The transmission process is modeled as a semi-Markov process, in fact the time spent in each state depends on what happens in the channel meanwhile, as it may be idle, used for a successful transmission, or shared by colliding STAs. The original model was proposed for omnidirectional communication, so that each STA is aware of ongoing transmissions and can defer its own when it senses the channel to be busy; thus collisions only happen when multiple STAs access the channel simultaneously because their backoff counters expired (at least two STAs are in a state $(\cdot, 0)$).

In the case of directional communication, instead, STAs may not detect ongoing transmissions, resulting in a much higher collision probability. In this work, we assume that the RTS/CTS mechanism is used, and that a STA always has both its transmitting and receiving antennas towards the AP, since it communicates only with it. We highlight that omnidirectional transmission in 802.11ad is highly discouraged [1] because it leads to a very short coverage range and farther STAs may not even be able to communicate with the AP. The AP

instead listens to the channel in a QO mode, as it does not know a priori which STA is going to start a communication. Upon successfully receiving an RTS, the AP switches its antenna configuration to point towards the STA that sent it. Fig. 2 shows the beam direction during the phases of a communication between a STA and the AP, which can be heard only by few other STAs. In fact, assuming the Line of Sight (LoS) component to be dominant,² the power P_{rx} received at a STA is:

$$P_{rx} = P_{tx} \frac{g_{tx}(\theta_{tx}, \varphi_{rx})g_{rx}(\theta_{rx}, \varphi_{tx})}{Ad^\eta}, \quad (1)$$

where P_{tx} is the power used to transmit, d is the distance from the transmitter, η is the path-loss exponent, $A = (4\pi/\lambda)^2$ is a normalizing path-loss term that depends on the wavelength λ , and g_{tx} and g_{rx} are the antenna gains of the transmitter and receiver, respectively, and depend on the angle of departure θ_{tx} and angle of arrival φ_{rx} of the signal. If the gains are very small, P_{rx} may be too low in order for the receiver to decode the signal properly.

STAs clustering. Our goal is to identify which STAs can detect an ongoing communication based on their positions so as to group STAs with the same characteristics. Consider a network consisting of n STAs, with a target STA S that communicates with the AP, so that S and the AP point to each other and the antenna gain in that direction is maximum. It is possible to cluster the other $n - 1$ STAs into four groups:

- $n_{I,1}$: STAs that can detect only the uplink messages from S to the AP.
- $n_{I,2}$: STAs that can detect only the downlink messages from the AP to S .
- $n_{I,3}$: STAs that can overhear the whole communication between the AP and S .
- $n_{I,4}$: STAs that cannot overhear any messages exchanged between the AP and S .

Note that these groups depend on the received power (see (1)), and therefore on the beam model (that influences the gains), thus may vary across transmissions.

Analogously, from the perspective of a STA S that listens to the channel, the other STAs can be divided into four groups: $n_{O,1}$ (S can overhear only the uplink messages from these STAs to the AP), $n_{O,2}$ (S can overhear only the downlink messages from the AP to these STAs), $n_{O,3}$ (S can detect all the messages exchanged between these STAs and the AP), and $n_{O,4}$ (S cannot detect any message exchanged between the AP and these STAs).

Points of collision. Collisions can happen at 3 different stages of the communication from a STA S to the AP, which can be visualized in Fig. 3.

- 1) S accesses the channel to transmit its RTS, but collides for sure. This can happen for three different reasons: i) if any other STA accesses the channel at the same time, as in legacy WiFi, ii) if a STA belonging to groups $n_{O,2}$ or $n_{O,4}$ is transmitting the RTS to the AP, or iii) if a STA in group $n_{O,4}$ has already sent the RTS and is

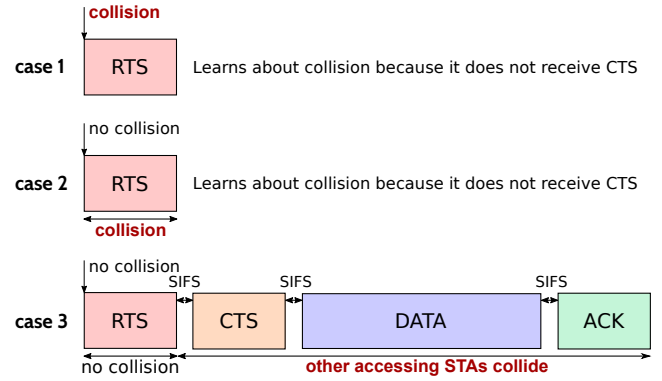


Figure 3: Stages of a message exchange between a STA and the AP depending on the collision point.

going on with the communication with the AP. Notice that, in the last case, S 's transmission fails, because the AP is listening in the direction of the STA from group $n_{O,4}$.³ The ongoing data transmission, instead, may still be successful, as directionality highly attenuates the interference and thus S 's transmission may not interfere. In this work, we assume that, except for channel errors, the ongoing data transmission is successful.

- 2) If none of the previous conditions happened, the transmission of the RTS may still be vulnerable to interference. In fact, if a STA in groups $n_{I,2}$ or $n_{I,4}$ accesses the channel meanwhile, the packets will collide.
- 3) If the transmission of the RTS was successful, the AP sends the CTS to S , which can then transmit its data. However, a STA in group $n_{I,4}$ is unaware of the ongoing communication and may try to access the channel, thus experiencing a collision. As assumed in case 1)iii), the outcome of the ongoing transmission only depends on channel errors.

We now propose an adaptation of Bianchi's model that accounts for directionality, assuming that the regions corresponding to the four groups of nodes are known; Sec. VI introduces an analytical model to compute such regions when constant-gain beam shapes are used.

B. Rethinking Bianchi's model

Bianchi's model [4] needs three major adaptations in order to be suitable for 802.11ad, which are caused by the following features.

- 1) CBAPs can be interrupted because there is a scheduled SP or the current DTI ends and thus the BHI of the next BI follows. In this case, all backoff counters have to freeze [1]; they will be restored in the next CBAP. This affects the time that a STA spends in a state (i, k) , $k \in \{1, \dots, W_i - 1\}$ before decrementing its backoff counter and transitioning to $(i, k - 1)$; the transition probability from (i, k) to $(i, k - 1)$ is 1 as in Bianchi's original model. We denote the freezing probability as p_f .
- 2) The finite duration of CBAPs may also cause transmissions deferral. In fact, if the backoff counter of a STA

²Although multipath plays a significant role in mmWave communication, this is out of the scope of this paper and left for future investigation.

³Different considerations can be made when considering Multiple-Input Multiple-Output (MIMO) systems.

reaches 0 but there is not enough time to complete a transmission, that STA should refrain from transmitting. The standard [1] however does not specify how to handle the backoff counter in this case. We decided to use the same approach used in [11], where a new backoff counter is randomly chosen from the current window (no collision happened). This causes the addition of new transitions from state $(i, 0)$ to (i, k) , $k \in \{0, \dots, W_i - 1\}$.⁴ We denote the probability of insufficient time in the current CBAP as timeout probability p_t .

- 3) The directional nature of mmWave communication has a huge impact on the operation of the DCF. It modifies the collision probability and the time spent in each state, which depend on the behavior of STAs whose transmissions can be detected by the target STA.

Fig. 4 represents the embedded MC of the semi-Markov process that we propose to model the transmission behavior of a STA during CBAP operation.

As in Bianchi's model, a state (i, k) , $i \in \{0, \dots, m\}$, $k \in \{0, \dots, W_i - 1\}$ refers to the i^{th} backoff stage with the backoff counter being equal to k . Here, m is the maximum number of retransmissions. The contention window in stage i is $W_i = \min\{2^i W_0, 2^m W_0\}$, where the initial window W_0 and the maximum window $2^m W_0$ are defined in the standard.

From a state (i, k) , $k > 0$, the backoff counter is decremented with probability 1 (solid black transitions in Fig. 4), but the time needed to transition to the next state $(i, k - 1)$ is variable, depending on how the channel is being used. When it reaches a state $(i, 0)$, the STA might be constrained to defer its transmission (adaptation 2). The average duration of a CBAP in the BI is $T_{\text{CBAP}}/N_{\text{CBAP}}$. We can assume that the probability of being in any time instant of the current allocation is uniform within the allocation, thus that the residual time in the current CBAP is uniformly distributed in $[0, T_{\text{CBAP}}/N_{\text{CBAP}}]$, as done in [10] and [11]. Then, the probability that there is no sufficient time to complete a transmission of duration T_L can be approximated as

$$p_t = \frac{T_L}{T_{\text{CBAP}}/N_{\text{CBAP}}}. \quad (2)$$

Thus, from each state $(i, 0)$, $i \in \{0, \dots, m\}$, the MC transitions to a state (i, k) , $k \in \{0, \dots, W_i - 1\}$ with probability p_t/W_i (dotted orange transitions in Fig. 4), while with probability $1 - p_t$ the STA accesses the channel. We identify the latter

⁴Another possibility is that the STAs whose backoff counter expired in the last fraction of the current CBAP allocation transmit as soon as the EDCA operation starts again. However, such approach may easily lead to collisions: if the counters of multiple STAs expire, all such STAs will attempt accessing the channel simultaneously in the next CBAP.

condition as being in a *transmission state* (the MC is in a state $(i, 0)$ and attempts to transmit); when the former condition applies (transmission deferral) or the MC is in a state (i, k) , $k > 0$, we say that the STA is in a *non-transmission state*. Note that transmission states do not coincide with states $(i, 0)$, $i \in \{0, \dots, m\}$, because the condition of no timeout (which happens with probability $1 - p_t$) needs to be verified as well. As in [5], each transmission state is itself a MC, which will be described in Sec. IV-C; thus, in order not to generate confusion, we will refer to the MC of Fig. 4 as *macro MC*.

Transmission attempts may result in failure, because of collisions with other transmissions (see the discussion in Sec. IV-A) or channel impairments. Let p be the total failure probability. In case of failure, the STA increments its collision counter and randomly selects a backoff counter based on the new contention window size, otherwise, in case of success, it proceeds with a new packet. Thus, from state $(k, 0)$ the MC goes to a state $(0, i)$, $i \in \{0, \dots, W_0 - 1\}$ (successful transmission of a new packet; solid green transitions in Fig. 4) with probability $(1 - p_t)(1 - p)/W_0$, or to any state $(k + 1, i)$, $i \in \{0, \dots, W_{k+1} - 1\}$ with probability $(1 - p_t)p/W_{k+1}$ (dashed red transitions in Fig. 4). If it reaches the maximum number of retransmission attempts ($k = m$), the MC goes from state $(m, 0)$ to a state $(0, i)$, $i \in \{0, \dots, W_0 - 1\}$ with probability $(1 - p_t)/W_0$. Note that this transition includes two distinct cases: the successful case where the packet is correctly received by the AP, which happens with probability $p(1 - p_t)$, and the failed case due to a collision, which happens with probability $(1 - p)(1 - p_t)$. In the previous retransmission stages this latter case led to a new stage, but here, since the retransmission counter has already reached its threshold m , the packet is discarded in favor of a new one. The two cases are represented with a single transition in the MC of Fig. 4.

The steady-state probabilities $\{b_{i,k} : i \in \{0, \dots, m\}, k \in \{0, \dots, W_i - 1\}\}$ of the macro MC can be computed using the same approach of [4]. Having $p_t < 1$, it is

$$b_{i,k} = \frac{W_i - k}{W_i} p b_{0,0}, \quad (3)$$

where $b_{0,0}$ is given in (4).

Notice that $b_{0,0}$ does not depend on p_t , which, nonetheless, has an impact on the delay. The case $p_t = 1$ makes no sense, because it corresponds to CBAP allocations so short that do not allow the transmission of any packet.

The probability of being in a transmission state is then

$$\tau = \sum_{i=0}^m b_{i,0}(1 - p_t) = \frac{1 - p^{m+1}}{1 - p} (1 - p_t) b_{0,0}, \quad (5)$$

$$b_{0,0} = \begin{cases} \frac{2(1 - 2p)(1 - p)}{W_0(1 - (2p)^{m+1}(1 - p) + (1 - p^{m+1})(1 - 2p))} & \text{if } m \leq m' \\ \frac{2(1 - 2p)(1 - p)}{W_0(1 - (2p)^{m'+1}(1 - p) + 2^{m'} W_0(p^{m'} - p^m)(1 - 2p)p + (1 - p^{m+1})(1 - 2p))} & \text{if } m > m' \end{cases} \quad (4)$$

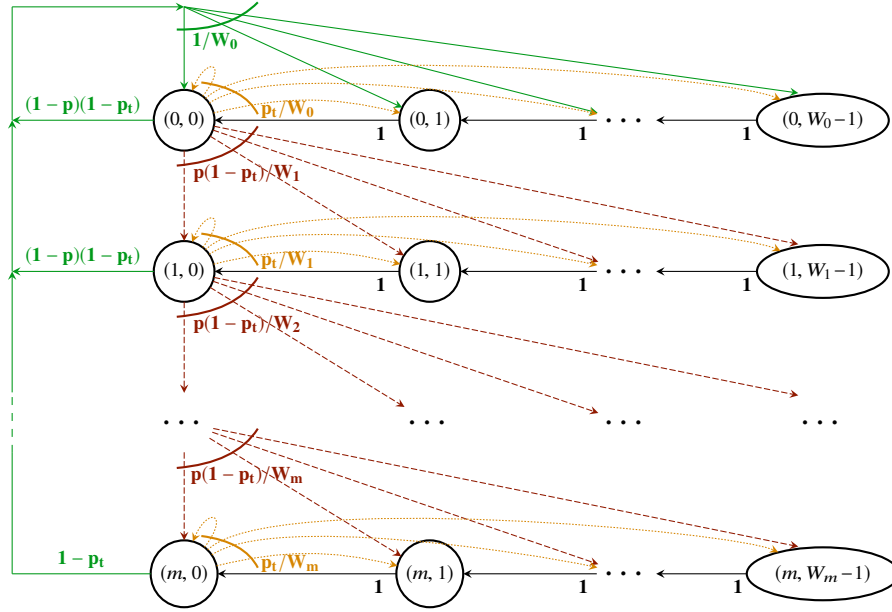


Figure 4: Macro Markov chain (adaptation of Bianchi's model [4]): embedded MC of the semi-Markov process.

where factor $1-p_t$ accounts for the probability of not deferring a transmission due to the shortage of time in the current CBAP allocation, as explained previously.

The time spent, on average, in a transmission or non transmission state is denoted as $E[T_{tx}]$ and $E[T_{ntx}]$, respectively, which depend on the probabilities $\{b_{i,k}\}$ as explained next. It is then possible to define the probability π_{tx} that, in an arbitrary time instant, the macro MC is in a transmission state:

$$\pi_{tx} = \frac{\tau E[T_{tx}]}{\tau E[T_{tx}] + (1-\tau)E[T_{ntx}]} \quad (6)$$

where τ is defined in (5). With probability $1-\pi_{tx}$, in an arbitrary time instant, the MC will be in a non transmission state. Note that (6) refers to the semi-Markov model, while (5) to the corresponding embedded MC. To derive $E[T_{tx}]$ and $E[T_{ntx}]$, we first need to understand what happens in a transmission state.

C. A transmission state

Whenever a STA is in a transmission state $(i, 0)$, $i \in \{0, \dots, m\}$, it attempts to transmit and enters a transmission state with probability $1-p_t$, while with probability p_t it picks a new backoff counter from the same window W_i (see Eq. (2)).

To model what happens during a transmission attempt, each transmission state forms its own MC, similarly to the approach in [5]. This nested MC is made of 6 states, as shown in Fig. 5: the *access* state A , the *collided RTS* state R_c , the *vulnerable RTS* state R_v , the *ongoing transmission* state O , the *failure* state F , and the *success* state S . A STA enters state A when it accesses the channel and goes from the macro MC into the transmission state MC. It starts to transmit the RTS, and, based on the discussion in Sec. IV-A, two cases can occur.

- As soon as the STA accesses the channel, it may immediately collide (case 1 in Sec. IV-A and in Fig. 3). This happens with probability $p_{c,1}$; in this case, the STA transitions to state R_c where it transmits the RTS and then, with probability 1, goes to the failure state F .

- Otherwise, the transmission of the RTS is still vulnerable to interference. If it collides (case 2 of Sec. IV-A and in Fig. 3), the MC transitions to the failure state F ; this happens with probability $p_{c,2}$. Otherwise, the STA goes to state O , where it receives the CTS from the AP and then sends its data.⁵ In turn, the data transmission may fail because of channel errors (but not because of interference, as assumed in Sec. IV-A) and therefore, with probability p_e , the next state in the MC is F . Otherwise, the transmission is successful and the next state in the MC is S . Then, from either F or S , the STA exits the transmission state.

Let b_j be the steady-state probability that the MC is in state $j \in \mathcal{J}_{tx} \triangleq \{A, R_c, R_v, O, F, S\}$. The transmission state itself forms a MC where the outgoing transitions from states S and F re-enter the transmission state from state A . Thus, the steady-state probabilities are: $b_A = 1/b_{tx}$, $b_{R_c} = (1-p_{c,1})/b_{tx}$, $b_{R_v} = p_{c,1}/b_{tx}$, $b_O = (1-p_{c,1})(1-p_{c,2})/b_{tx}$, $b_F = (1-(1-p_{c,1})(1-p_{c,2})(1-p_e))/b_{tx}$, $b_S = (1-p_e)(1-p_{c,1})(1-p_{c,2})/b_{tx}$, where $b_{tx} = 3 + (1-p_{c,1})(1-p_{c,2})$.

Similarly to what done for the macro MC, we differentiate between the probabilities of the embedded MC and those of the semi-Markov model. We define as π_j the probabilities that, in an arbitrary time instant, the MC is in state $j \in \mathcal{J}_{tx}$, given that the MC is in a transmission state:

$$\pi_j = \frac{T_j b_j}{\sum_{\ell \in \mathcal{J}_{tx}} T_\ell b_\ell} \quad j \in \mathcal{J}_{tx}, \quad (7)$$

where T_j is the average time spent in state j . The error probability p_e instead depends on the Signal-to-Noise-Ratio (SNR) and the Modulation and Coding Scheme (MCS) used.

D. Collision probabilities

In Sec. IV-A we explained that we group STAs based on what messages they can detect over the channel, and

⁵No collisions can happen during the transmission of the CTS and we assume that there are no packet errors.

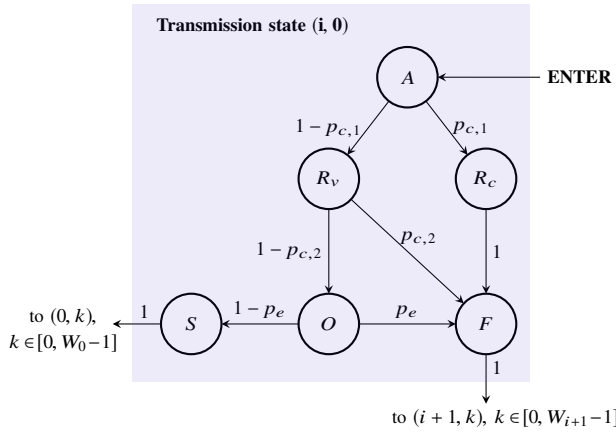


Figure 5: Markov chain that models a transmission state. It is entered from i) state $(i, 1)$ with probability $1 - p_t$, ii) state $(i - 1, 0)$ with probability $p(1 - p_t)/W_{i-1}$ or iii) state $(i, 0)$ itself with probability p_t/W_i .

thus which information about the channel occupancy they have available. In this section, we characterize the collision probabilities $p_{c,1}$ and $p_{c,2}$ (see Fig. 4) depending on such information.

Probability $p_{c,1}$. A STA will collide upon accessing the channel if another STA is accessing the channel in that exact moment (as happens with legacy WiFi) or if the channel is already in use but this information is hidden to that STA. Thus, $p_{c,1}$ is given by the probability that *at least* one of the following three events occurs: i) any of the other STAs accesses the channel simultaneously, ii) at least a STA in group $n_{O,2}$ is transmitting an RTS to the AP, or iii) at least a STA in group $n_{O,4}$ is using the channel. We denote as q_1 , q_2 and q_3 the probabilities of these events, and, for mathematical tractability, we approximate them as independent of each other. The probability of collision is thus

$$p_{c,1} = 1 - (1 - q_1)(1 - q_2)(1 - q_3). \quad (8)$$

We now analyze these events.

Case i) occurs if at least another STA is accessing the channel, given that S is accessing the channel. By using Bayes rule, the probability that this happens can be expressed as the probability that at least two STAs are accessing the channel over the probability $p_{acc} = \pi_A \pi_{tx}$ that a STA is accessing the channel:

$$q_1 = \frac{1 - (1 - p_{acc})^n - n p_{acc} (1 - p_{acc})^{n-1}}{p_{acc}}, \quad (9)$$

where n is the total number of STAs in the network and the numerator represents the probability that at least two out of n STAs are accessing the channel.

Case ii) happens if at least a STA in group $n_{O,2}$ is either in state R_v or in R_c , given that S is accessing the channel. In such condition, in fact, S is unaware of the ongoing communications of STAs in groups $n_{O,2}$ because it cannot detect their uplink messages and the AP has not replied yet. Thanks to Bayes' rule, the probability that this occurs can be equivalently expressed as a function of the probability that S accesses the channel given that at least a STA in group $n_{O,2}$ is either in state R_v or in R_c . This is not trivial to compute, because it requires an analytical expression for the relations between the coverage areas of multiple STAs. In fact, if a STA

in group $n_{O,2}$ entered a transmission state, all STAs that can hear it refrain from transmitting, so that fewer STAs compete for the channel and S more likely senses the channel as idle and attempts transmitting. However, we do not consider such relations, which are extremely challenging to model, but only account for the fact that, if some STAs are in a transmission state, the EDCA operation is not frozen. The access probability is thus increased by a factor $1/(T_{CBAP}/T_{BI})$. We express the probability of case ii) as

$$q_2 = \frac{1 - (1 - \pi_{tx}(\pi_{R_v} + \pi_{R_c}))^{n_{O,2}}}{T_{CBAP}/T_{BI}}. \quad (10)$$

The numerator represents the probability that none of the STAs in group $n_{O,2}$ is in state R_v or R_c , while the denominator is the normalization factor we introduced. As the numerical evaluation of Sec. VII shows, this approximation affects the validity of the model only for highly dense scenarios, with more than 100 STAs.

Case iii) happens if at least a STA in group $n_{O,4}$ is in any of the transmission states R_v , R_c , O , given that S is accessing the channel, because S cannot detect any of the messages they exchange with the AP. This event can be treated analogously to case ii) and thus happens with probability

$$q_3 = \frac{1 - (1 - \pi_{tx}(\pi_{R_v} + \pi_{R_c} + \pi_O))^{n_{O,4}}}{T_{CBAP}/T_{BI}}. \quad (11)$$

Probability $p_{c,2}$. If S collided during channel access, it goes to state R_c , meaning a certain failure. Otherwise, it enters state R_v . Here, it is still vulnerable to collisions: it in fact collides if at least a STA that cannot detect the uplink messages sent by S (groups $n_{I,2}$ and $n_{I,4}$) accesses the channel while S is in R_v , i.e., for the whole duration T_{R_v} (according to discrete intervals with the duration T_A of a channel access attempt). Following the same reasoning as per (10) and (11), this happens with probability

$$p_{c,2} = \frac{1 - ((1 - p_{acc})^{n_{I,2} + n_{I,4}})^{T_{R_v}/T_A}}{T_{CBAP}/T_{BI}}. \quad (12)$$

Probabilities computation. Eqs. (7), (8), (12) form a non-linear system in the unknowns π_j , $p_{c,1}$ and $p_{c,2}$, which can be solved using numerical techniques, as in Bianchi's original model.

V. PERFORMANCE METRICS

We evaluate the performance achievable in a CBAP in terms of throughput, drop rate, and delay. Before that, we derive the time spent in a transmission and non transmission state.

A. Average time spent in a transmission state

A STA that accesses a transmission state can follow 4 different paths, depending on collisions and errors. This can be easily seen in Fig. 5. The average time spent in a transmission

state is the sum of the time associated to each of these paths, weighed by the probability of that path:

$$\begin{aligned} E[T_{\text{tx}}] &= (T_A + T_{R_c} + T_F)p_{c,1} \\ &+ (T_A + T_{R_v} + T_O + T_F)(1 - p_{c,1})(1 - p_{c,2})p_e \\ &+ (T_A + T_{R_v} + T_F)(1 - p_{c,1})p_{c,2} \\ &+ (T_A + T_{R_v} + T_O + T_S)(1 - p_{c,1})(1 - p_{c,2})(1 - p_e). \end{aligned} \quad (13)$$

The probabilities π_j are defined in (7) and the times T_j are as follows: $T_A = \delta$, $T_{R_c} = RTS$, $T_{R_v} = RTS$, $T_O = CTS + E[T_L] + ACK + 3SIFS + 3\delta$, $T_F = DIFS$, $T_S = DIFS$, where δ is the propagation delay, RTS and CTS represent the time needed to send an RTS and CTS message, respectively, $E[T_L]$ is the average time needed to transmit a data packet, ACK is the time to send an ACK, and $SIFS$ and $DIFS$ represent the Short Interframe Space (SIFS) and DIFS durations, respectively [1].

B. Average time spent in a non-transmission state

The time spent in a non-transmission state depends on what happens meanwhile: the CBAP may freeze, and S may hear a transmission or sense the channel as idle. The EDCA mechanism assumes that the backoff counter is decremented only after the channel is sensed idle for a time slot of duration σ (which is defined in the standard and depends on the PHY layer). Before that, the CBAP may freeze or be busy. We can interpret the freezing condition as a self-loop on a state (i, k) , $k > 0$ with probability

$$p_f = 1 - \frac{T_{\text{CBAP}}}{T_{\text{BI}}}, \quad (14)$$

so that on average $1/(1-p_f)$ iterations over (i, k) are expected before a transition to $(i, k-1)$.

S senses the channel as idle when i) none of the STAs in $n_{I,1}$ and $n_{I,3}$ is using the channel, and ii) none of the STAs is using the channel *and* has already received a feedback from the AP:

$$p_i = (1 - \pi_{\text{tx}}(\pi_A + \pi_{R_c} + \pi_{R_v} + \pi_O))^{n_{I,1} + n_{I,3}} (1 - \pi_{\text{tx}}\pi_O)^{n_{I,2}}, \quad (15)$$

The channel is sensed as busy with probability $1 - p_i$ for an average duration of E_{tx} . Thus, the average time spent in a non-transmission state can be expressed as

$$E[T_{\text{ntx}}] = \sigma + \frac{(1 - p_i)E_{\text{tx}}}{1 - p_f}. \quad (16)$$

C. Throughput

The normalized system throughput U is defined as the fraction of time that the channel is used to successfully transmit information. The average payload size is $E[L]$ and a transmission is successful with probability $\pi_{\text{tx}}(1 - p)$. Thus the aggregated throughput is

$$U = n \frac{\pi_{\text{tx}}(1 - p)E[L]}{\pi_{\text{tx}}E[T_{\text{tx}}] + (1 - \pi_{\text{tx}})E[T_{\text{ntx}}]}, \quad (17)$$

where the denominator represents the average duration of a time slot.

D. Drop rate

A packet is dropped when the sender fails all its transmission attempts for the packet, i.e., the packet transmission fails at all the stages $0, 1, \dots, m$. This happens with probability $p_{\text{drop}} = p^{m+1}$. Clearly, the larger p , the larger the drop probability.

Another metric of interest is the average number of transmission attempts per packet, denoted as $E[n_{\text{tx}}]$. We introduce $\Pr(\text{TX}(i)) = (1 - p)p^i$, which represents the probability of a successful transmission at stage i . Then, $E[n_{\text{tx}}]$ can be expressed as

$$\begin{aligned} E[n_{\text{tx}}] &= \sum_{i=0}^m (i + 1) \Pr(\text{TX}(i)) + (m + 1)p_{\text{drop}} \\ &= \sum_{i=0}^m (i + 1)(1 - p)p^i + (m + 1)p^{m+1} \\ &= \frac{1 - (m + 2)p^{m+1} + (m + 1)p^{m+2}}{1 - p} + (m + 1)p^{m+1} \\ &= \frac{1 - p^{m+1}}{1 - p}, \end{aligned} \quad (18)$$

where the term $(m+1)p_{\text{drop}}$ stands for the transmission attempts made for a dropped packet.

If we want to consider the average number of transmission attempts only per successfully delivered packets, we have to neglect this contribution and also condition the probability $\Pr(\text{TX}(i))$ to the fact that the packet was successfully delivered. The event success happens when the packet is not discarded after m backoff stages, i.e., with probability $\Pr(\text{success}) = 1 - p_{\text{drop}}$. Thus:

$$\begin{aligned} E[n_{\text{tx}}|\text{success}] &= \sum_{i=0}^m (i + 1) \Pr(\text{TX}(i)|\text{success}) \\ &= \sum_{i=0}^m (i + 1) \frac{\Pr(\text{success}|\text{TX}(i)) \Pr(\text{TX}(i))}{\Pr(\text{success})} \\ &= \sum_{i=0}^m (i + 1) \frac{(1 - p)p^i}{1 - p^{m+1}} \\ &= \frac{1 - (m + 2)p^{m+1} + (m + 1)p^{m+2}}{(1 - p)(1 - p^{m+1})}, \end{aligned} \quad (19)$$

where we accounted for the fact that $\Pr(\text{success}|\text{TX}(i)) = 1$.

E. Delay

The delay experienced by a (successfully transmitted) packet is the time elapsed from when it arrived at the MAC layer until it is received, and can be computed using an analogous approach to that in [10]. Let $E[D_i]$ denote the expected delay that a packet experiences when it is successfully transmitted at stage i . Then

$$E[D] = \sum_{i=0}^m \Pr(\text{TX}(i)|\text{success})E[D_i], \quad (20)$$

where $\Pr(\text{TX}(i)|\text{success})$ represents the probability that, given that a successful transmission happened, it was at stage i . From (19) we know that $\Pr(\text{TX}(i)|\text{success}) = (1 - p)p^i / (1 - p^{m+1})$.

p^{m+1}). The term $E[D_i]$ is the sum of the average backoff process delay in stages $0, 1, \dots, i$, the collision delay experienced in stages $0, 1, \dots, i-1$, and the time needed for the successful transmission at stage i . The first state k in the j^{th} backoff stage is uniformly distributed between 0 and $W_j - 1$; the counter is decremented until state $(j, 0)$ ($k+1$ states are crossed) and then, with probability p_t there is a transition back to a random state at stage j . Therefore, the delay term is:

$$\begin{aligned} E[D_i] &= iT_c + T_s + E[T_{\text{ntx}}] \sum_{j=0}^i \sum_{\ell=0}^{+\infty} p_t^\ell \sum_{k=0}^{W_j-1} \frac{k+1}{W_j} \\ &= iT_c + T_s + \frac{E[T_{\text{ntx}}]}{1-p_t} \sum_{j=0}^i \frac{W_j+1}{2} \end{aligned} \quad (21)$$

where $E[T_{\text{ntx}}]$ is the time spent in a backoff state and T_c and T_s are the durations of a successful transmission and a collision, respectively:

$$T_s = RTS + CTS + E[T_L] + ACK + 3SIFS + 4\delta, \quad (22)$$

$$T_c = RTS + DIFS + \delta. \quad (23)$$

Observation 1. Some papers in the literature (e.g., [10], [12]) consider CBAP allocations to be used by a single sector around the PCP/AP at a time, in a round-robin fashion. Such assumption has a strong impact on the network performance, but since it is not specified by the standard [1], we chose not to use it and leave it for future work. Note that, however, it would require only a slight modification in our model.

Observation 2. In this first study, we decided to neglect occlusion, which may cause blockage and packet loss. This phenomenon could be integrated in the proposed framework by appropriately modifying the collision probability. This however would require a detailed study of the statistical distribution of the occlusion events as well as their impact, based also on the propagation environment, and cannot be included in the present paper due to lack of space. This interesting analysis is therefore left for future investigation.

VI. A MODEL FOR DIRECTIONAL COMMUNICATION

The model of Sec. IV-A assumes to know the number of STAs that can overhear the uplink and downlink messages exchanged between the AP and a target STA, which is equivalent to characterizing the regions around the target STA corresponding to groups $n_{I,1}$, $n_{I,2}$, $n_{I,3}$ and $n_{I,4}$. This is not trivial to compute as the power received at a STA depends on the gains of the transmitting and receiving antennas, as per (1), which vary according to the considered direction (angles θ_{tx} and φ_{rx} in (1)). We however want to stress that the model of Sec. IV-A is of general validity and can be applied to different beam shape models, as regions can also be determined using a numerical approach or through simulation, rather than with a closed-form expression. In the following, we describe the model we use for the beam shapes and then provide a mathematical approach to compute the areas corresponding to each group of STAs.

A. Beam shapes

The directivity of an antenna depends on the shape of a beam. There exist a multitude of models for antenna beams, such as the Gaussian beam shape, the sinc beam shape and the sampled beam shape, which, however, are very challenging to be used in mathematical models. A simpler approach is given by the constant-gain beam shape, where the space around the device is divided into N_b beams with constant beamwidth $W_b = 2\pi/N_b$; a beam has constant gain in the main lobe and there are no side lobes. From the expression of the directivity of an antenna [19], the antenna gain for a beam centered at φ is $g(\theta) = N_b$ if $\theta \in \left[\varphi - \frac{W_b}{2}, \varphi + \frac{W_b}{2}\right]$, and 0 otherwise.

We assume homogeneous STAs with the same antenna gains; however, it makes sense to consider the AP to be more powerful than the STAs and with narrower beams. We denote as N_{AP} and N_{S} the number of sectors for the AP and a STA, respectively, and assume $N_{\text{AP}} \geq N_{\text{S}} \geq 2$.

As explained in Sec. IV-A, since the STAs only communicate with the AP, they always have their transmitting and receiving antennas directed towards it. The AP instead listens in a QO mode and switches to directional mode when engaged in a communication with a STA, after successfully receiving its RTS. In this work, we assume that the QO mode coincides with omnidirectionality and yields a unit gain.

We also assume full transmitter/receiver reciprocity, meaning that a STA uses the same sector to transmit to and receive from the AP, and vice versa. The antenna gains of the AP and STA in directional mode computed with the model in Sec. VI-A are $g_{\text{AP}} \equiv N_{\text{AP}}$ and $g_{\text{S}} \equiv N_{\text{S}}$ in the main lobes, respectively, and zero outside (see Fig. 6).

B. Coverage area and power regulations

Since there are no side lobes, two STAs can hear each other only if they are in each other's main lobe, respectively. Given this and considering the average, it is possible to derive a maximum transmission range by means of a threshold γ_{th} on the SNR $\gamma = P_{\text{rx}}/N$, where N is the noise power. Then, using (1), the distance d between two devices should be

$$d = \left(\frac{P_{\text{tx}} g_{\text{tx}}(\theta_{\text{tx}}, \varphi_{\text{rx}}) g_{\text{rx}}(\theta_{\text{tx}}, \varphi_{\text{rx}})}{\gamma_{\text{th}} AN} \right)^{1/\eta}. \quad (24)$$

The threshold γ_{th} can be computed by imposing a maximum tolerable Bit Error Rate (BER) and deriving the corresponding SNR (note that this depends on the MCS used). The antenna gains of the AP and STA are computed as described in Sec. VI-A. The transmission power, instead, is subject to restrictions that vary from country to country; see, e.g., the Federal Communication Commission (FCC)⁶ and European Telecommunications Standards Institute (ETSI)⁷ regulations for the US and Europe, respectively, which state limits on the Equivalent Isotropic Radiated Power (EIRP). In this work, we assume a full channel with flat Power Spectral Density (PSD), so that a 10 W (corresponding to 40 dBm) limit on the

⁶<https://www.fcc.gov/document/part-15-rules-unlicensed-operation-57-64-ghz-band>

⁷https://www.etsi.org/deliver/etsi_en/302500_302599/302567/02.00.22_20/en_302567v020022a.pdf

EIRP and 500 mW (corresponding to 27 dBm) of maximum fed power satisfy both the FCC and the ETSI regulations. In general, it is suggested that the most directive sector with gain maxGain should be the one limiting the power. We thus choose

$$P_{\text{tx}} = \min\{27 \text{ dBm}, 40 \text{ dBm} - \text{maxGain}\}. \quad (25)$$

In our case, maxGain coincides with the number of antenna sectors. Note that for maxGain < 13 dB, i.e., number of sectors lower than 20, Eq. (25) yields a transmission power of 27 dBm. The maximum distance between a STA and the AP is therefore limited by their antenna directivities.

Interestingly, if the AP and the STA have different transmission powers, there is an SNR asymmetry between downlink and uplink when considering the same noise level at the receiver and the transmitter (see (1) and (24)). We assume the coverage radius R to be bounded by the most stringent limit (24) between uplink (P_{tx} and g_{tx} are those of the STA, g_{rx} is that of the AP which can be listening in either QO or directional mode) and downlink communication (P_{tx} and g_{tx} are those of the AP, g_{rx} is that of the STA). Then, we consider an area $\mathcal{R} = \pi R^2$ around the AP with the STAs uniformly distributed according to a Poisson Point Process (PPP) of intensity λ .

C. Stations that overhear uplink messages

We consider a Cartesian plane whose origin coincides with the center of area \mathcal{R} , so that the AP is in $(0, 0)$. Without loss of generality, we assume that the target STA S is in $(d_t, 0)$, $d_t \leq R$. Considering the constant-beam model, the interferer can overhear uplink communication from S to the AP if it is in the main lobe of S and vice versa, otherwise the received power is 0 as per (1). Consider an interferer at distance $d_i \leq R$ from the AP. It can overhear the uplink communication if and only if the phase of its polar coordinates is in the range $[\varphi_{\text{lim}}(d_i), 2\pi - \varphi_{\text{lim}}(d_i)]$, where

$$\varphi_{\text{lim}}(d_i) = \begin{cases} \pi - \frac{\theta_S}{2} - \arcsin\left(\frac{d_i}{d_t} \sin\left(\frac{\theta_S}{2}\right)\right) & \text{if } d_i \leq d_t \\ \pi - \frac{\theta_S}{2} - \arcsin\left(\frac{d_t}{d_i} \sin\left(\frac{\theta_S}{2}\right)\right) & \text{if } d_i > d_t \end{cases} \quad (26)$$

The proof of this result is provided in Appendix A.

Considering all possible distances d_i , we obtain the expected area of STAs that can overhear uplink messages given the position of the target node $(d_t, 0)$ as

$$\begin{aligned} \mathcal{R}_R(d_t) &= \int_0^R \int_{\varphi_{\text{lim}}(d_i)}^{2\pi - \varphi_{\text{lim}}(d_i)} r \partial\theta r \partial r \\ &= \pi R^2 - 2 \int_0^R \varphi_{\text{lim}}(r) r \partial r = \pi R^2 \\ &\quad - 2 \int_0^{d_t} \left(\pi - \frac{\theta_S}{2} - \arcsin\left(\frac{r}{d_t} \sin\left(\frac{\theta_S}{2}\right)\right) \right) r \partial r \\ &\quad - 2 \int_{d_t}^R \left(\pi - \frac{\theta_S}{2} - \arcsin\left(\frac{d_t}{r} \sin\left(\frac{\theta_S}{2}\right)\right) \right) r \partial r \end{aligned} \quad (27)$$

which can be solved in closed form (which, nonetheless, does not provide any useful insight, so we are not providing the expression).

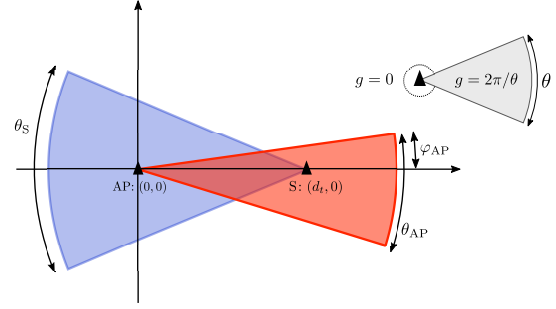


Figure 6: Location of the AP and the target STA S in the Cartesian plane. The red beam is the AP beam in the direction of S , has width θ_{AP} and goes from $\varphi_{\text{AP}} - \theta_{\text{AP}}$ to φ_{AP} ; the blue beam is S 's beam in the direction of the AP and has width θ_S . In the upper-right corner, example of constant-gain beam of width θ : the antenna gain is $2\pi/\theta$ within the beam, 0 outside.

The position of the target node is uniformly distributed within a circle of radius R centered in the AP, making the distance d_t distributed in the range $[0, R]$ with probability density function $f(d_t) = 2d_t/R^2$. Thus, the expected area of STAs that can hear uplink messages is given by averaging (27) over d_t :

$$\text{E}[\mathcal{R}_R] = \int_0^R \mathcal{R}_R(d_t) \frac{2d_t}{R^2} \partial d_t \quad (28)$$

which also can be solved in closed form and only depends on the beam width θ_S .

D. Stations that overhear downlink messages

Without loss of generality we keep assuming that the target STA is in $(d_t, 0)$, and consider it to be in a random angular position within the AP sector that covers it, which has width θ_{AP} . We thus denote as $\varphi_{\text{AP}} \in [0, \theta_{\text{AP}}]$ the angular phase of such sector, so that it spans the angles in the Cartesian plane in the range $[\varphi_{\text{AP}} - \theta_{\text{AP}}, \varphi_{\text{AP}}]$, as shown in Fig. 6. The covered area is

$$\mathcal{R}_C = \int_0^R \int_{\varphi_{\text{AP}} - \theta_{\text{AP}}}^{\varphi_{\text{AP}}} r \partial\theta r \partial r = \pi R^2 = \frac{\theta_{\text{AP}}}{2} R^2. \quad (29)$$

All STAs in that sector can overhear downlink communications from the AP to the target STA, and, in particular, the CTS. Note that $\text{E}[\mathcal{R}_C] \equiv \mathcal{R}_C$.

E. Stations that overhear both uplink and downlink messages

In this case, we have to consider the area that satisfies the requirements of both Secs. VI-C and VI-D. Thus

$$\mathcal{R}_{R,C}(d_t, \varphi_{\text{AP}}) = \int_0^R \left(\int_{\varphi_{\text{lim}}(r)}^{\varphi_{\text{AP}}} \partial\theta + \int_{\varphi_{\text{AP}} - \theta_{\text{AP}}}^{2\pi - \varphi_{\text{lim}}(r)} \partial\theta \right) r \partial r. \quad (30)$$

Notice that $\varphi_{\text{lim}}(\cdot)$ depends on the distance of the interferer from the AP. It is possible to obtain a closed form expression for (30), as explained in Appendix B.

Table I: Simulation parameters.

BI structure		
BI duration	BI	100 ms
BHI duration	BHI	2 ms
Number of CBAP allocations	N_{CBAP}	2
Sectors for directional communication [6]		
AP	N_{AP}	32
STA	N_S	4
EDCA parameters [1]		
Minimum contention window size	W_0	16
Maximum contention window size	$2^{m'}W_0$	1024
Maximum # retransmission attempts	m	6
Slot duration	σ	5 μ s
SIFS	$SIFS$	3 μ s
DIFS	$DIFS$	13 μ s
Propagation delay	δ	100 ns
Packets size [1]		
MAC header	H_{MAC}	320 b
PHY header	H_{PHY}	64 b
RTS size	L_{RTS}	20 * 8 b
CTS size	L_{CTS}	20 * 8 b
ACK size	L_{ACK}	14 * 8 b
Average data size	$E[L]$	7995 * 8 b - H_{MAC}
Noise		
Noise figure	F	10 dB
Bandwidth	W	2.16 GHz
Path loss exponent	η	2.5

The corresponding expected area of STAs that can overhear both uplink and downlink messages is obtained by averaging (30) over $d_t \in [0, R]$ and $\varphi_{AP} \in [0, \theta_{AP}]$:

$$E[\mathcal{R}_{R,C}] = \int_0^R \frac{2d_t}{R^2} \left(\int_0^{\theta_{AP}} \frac{1}{\theta_{AP}} \mathcal{R}_{R,C}(d_t, \varphi_{AP}) \partial\varphi_{AP} + \int_0^{\theta_{AP}} \frac{1}{\theta_{AP}} \mathcal{R}_{R,C}(d_t, \varphi_{AP}) \partial(\theta_{AP} - \varphi_{AP}) \right) \partial d_t. \quad (31)$$

Appendix B explains how to compute (31). Note that the integrals in (30) yield zero for some positions of the target STA and the interferers.

F. Classification of the stations

Given Eqs. (27)–(31), it is possible to quantify the regions $\mathcal{R}_\ell, \ell \in \{1, 2, 3, 4\}$ corresponding to the groups of nodes $n_{I,\ell}$ introduced in Sec. IV-A:

$$\begin{aligned} \mathcal{R}_1 &= E[\mathcal{R}_R] - E[\mathcal{R}_{R,C}] \\ \mathcal{R}_2 &= E[\mathcal{R}_C] - E[\mathcal{R}_{R,C}] \\ \mathcal{R}_3 &= E[\mathcal{R}_{R,C}] \\ \mathcal{R}_4 &= \mathcal{R} - \mathcal{R}_1 - \mathcal{R}_2 - \mathcal{R}_3. \end{aligned} \quad (32)$$

In this work, we assume that the STAs are distributed according to a PPP. Notice that, given the symmetry of the coverage areas, it is $n_{O,\ell} \equiv n_{I,\ell} \forall \ell$.

VII. NUMERICAL EVALUATION

We validated the proposed model by comparing its performance in terms of throughput and delay with that of realistic Monte Carlo simulations for different system configurations. In particular, we investigated the accuracy of the model as a

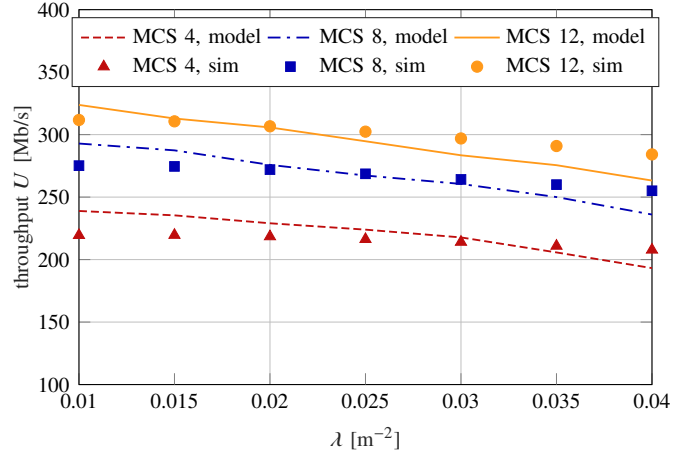


Figure 7: Throughput vs STA density. Analytical model and simulation for different MCSs when $\nu = 0.5$.

function of the fraction of DTI dedicated to CBAP allocations, the node density, and the MCS used.

The system parameters are summarized in Table I. The time spent to send a message depends on its size, the data rate of the MCS used and the duration of the PHY preamble. RTS, CTS and ACK messages are sent using the control modulation, which corresponds to a rate of 27.5 Mb/s [1]. For data transmission we assume to use the Single Carrier PHY layer, and in particular $MCS = 4, 8, 12$, which yield a nominal data rate of 1.16, 2.31 and 4.62 Gb/s, respectively [1].

We also set a maximum BER of 10^{-6} and mapped such requirement onto a threshold γ_{th} on the SNR.⁸ This allows to derive the area covered by the AP as per Sec. VI-A, where the antenna gains are derived from the number of antenna sectors, and the noise power is $N = kT_0FW$, where k is the Boltzmann constant and $T_0 = 290$ K; the noise figure F , the path loss exponent η and the bandwidth W are given in Table I. The chosen configuration corresponds to a circular area of radius $R = 26$ m and we analyze node densities up to 85 nodes.

Note that we assume a fixed MCS, while in real networks, STAs use rate adaptation to select the optimal MCS based on the link status. This enhancement is left for future investigation as our main goal here is to assess the performance in a more static configuration, which is a starting point for more realistic yet more complex scenarios.

Fig. 7 shows the aggregated throughput U (see Eq. (17)) as a function of the STA density λ (from about 20 up to more than 80 STAs in the network) for different choices of the MCS. We fixed the fraction of DTI devoted to CBAP to $\nu \triangleq T_{CBAP}/T_{DTI} = 0.5$, i.e., half of the DTI is used for contention-based access. The model provides a sufficiently reliable estimate of U , but tends to exacerbate a decreasing trend as a function of λ . This mismatch is due to the approximations introduced to compute the collision probabilities. We in fact assumed that the STAs access the channel independently, while, as discussed in Sec. IV-C, this is not true in reality

⁸We built an SNR-BER map using the WLAN ToolboxTM of MATLAB software, which provides functions for modeling the 802.11ad PHY.

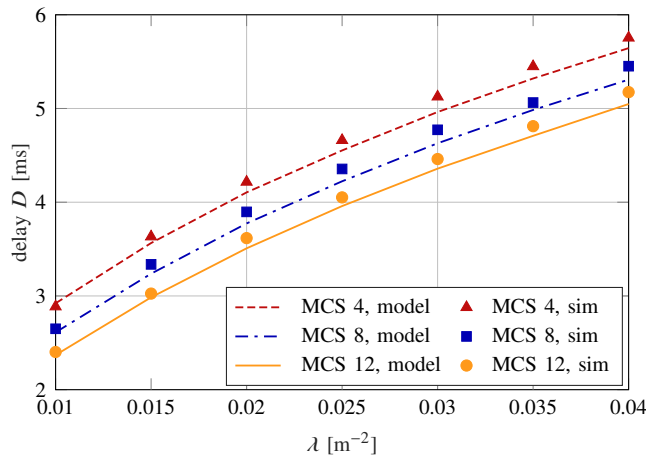


Figure 8: Delay vs STA density. Analytical model and simulation for different MCSs when $\nu = 0.5$.

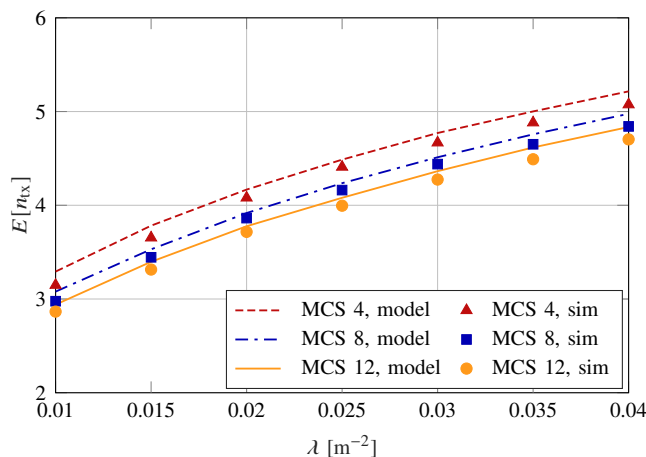


Figure 9: Average number of transmission attempts per packet vs STAs density when $\nu = 0.5$.

because the deafness and hidden node issues introduce correlation in the positions of the STAs that erroneously identify the channel as idle. The model is not able to capture this dependence among STAs and thus its results slightly deviate from the real performance. In addition, Fig. 7 shows that the STA density has only a marginal impact on the aggregated throughput: although the success rate of each STA considered separately decreases for larger values of λ , the number of STAs increases, yielding an almost constant value of U . Moreover, as expected, the throughput is basically proportional to the nominal data rate of the MCS.

Similar considerations can be made for the delay, shown in Fig. 8 for the same system setting of Fig. 7. The model slightly underestimates the delay, but fits well the behavior as λ and the MCS vary. Although the STA density has a marginal effect on the aggregated throughput, it does have an impact on the delay: the delay increases with the STA density because the higher collision rate leads to a larger number of retransmissions. Also, the more robust the MCS, the larger the delay, because data transmission takes longer. This effect

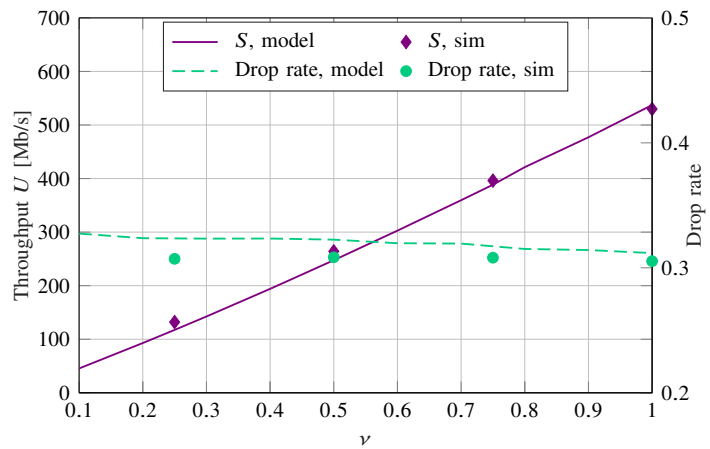


Figure 10: Throughput and drop rate vs CBAP fraction when $\lambda = 0.03$ and MCS = 8.

Figure 11: Delay vs CBAP fraction for different choices of λ when MCS = 8.

is also due to the fact that, with a stronger MCS, a higher number of transmission attempts is (on average) required to transmit a packet, as shown in Fig. 9. This latter result may sound counterintuitive, as stronger MCS should guarantee a larger success probability. However, this is not the case of our scenario, where the cell radius is such to cover even the largest MCS used in the numerical evaluation, and the MCS is not changed over different transmission attempts. Thus, in this scenario, a more robust MCS simply results in a longer transmission time, during which the other STAs may try to access the channel and collide, thereby increasing the number of transmission attempts. As expected, the number of transmission attempts (see Eq. (19)) increases with the STAs density.

In Figs. 10 and 11 we evaluated the impact of ν on throughput, drop rate, and delay, with MCS = 8. As discussed previously, there is a modest mismatch between simulations and model, which is most evident in the drop rate as it only depends on the collision probability and is not mitigated by other factors. The drop rate is shown in Fig. 10 for $\lambda = 0.03$ (more than 60 STAs) and is almost constant with respect to ν . The aggregated throughput instead increases proportionally with ν , because there is more time dedicated to CBAP (since U is not normalized to the CBAP duration). For the same reason, the delay (see Fig. 11) drops as ν increases: the EDCA operation is suspended less often and the timeout probability is reduced, allowing the transmission of more packets. Clearly, as Fig. 11 shows, the denser the network (i.e., the larger λ), the larger the delay, since the higher interference increases the collision probability.

Concluding, the proposed model provides results comparable to those obtained by simulations and, thus, can be used to easily analyze the impact of the system parameters on the performance obtainable in the CBAP allocations.

VIII. CONCLUSION

In this work, we proposed an analytical model for the CBAP allocations in 802.11ad networks. We adapted the seminal

model of Bianchi for legacy WiFi to account for the distinct features of the new amendment, including the interleaving of CBAP and SP allocations and the directional communication, which exacerbates the deafness and hidden node problems.

Assessing the performance that can be obtained in CBAPs is the first step to design an efficient scheduler and determine the DTI structure that better accommodates the traffic requirements of multiple STAs. Although the mathematical model slightly deviates from the real performance due to assumptions and simplifications, it is able to capture (at least qualitatively) the system behavior and can be extremely useful to plan the DTI scheduling and to gain insight on the impact of various parameters. In further analysis, we would like to relax some of the assumptions and study a more realistic scenario, e.g., by taking into account rate adaption and occlusion.

In our future work, we would like to characterize also the other types of allocations of 802.11ad, i.e., SPs and dynamic allocations, and merge such models to build an efficient scheduler. We also plan to investigate how our model can be modified to better capture/support the new features of 802.11ay [20], such as channel aggregation and MIMO. Moreover, we would like to analyze what happens if the area around the AP is divided into regions that participate in different rounds of the CBAP operation, or, more generally, when some STAs are not allowed to participate in a certain allocation.

Another interesting extension concerns the study of the potential benefits introduced by the RTS/CTS handshake in the presence of directional communication. These control messages could in fact go undetected by the other STAs and may even result in a higher interference. So, in some cases it may even be better not to use them at all, due to the associated overhead and latency. We would like to compare the network performance with and without RTS/CTS in the case of directional communication, to determine in which situations this mechanism is useful.

We remark that the model proposed in Sec. IV does not depend on the model used for the antenna beams, but for mathematical tractability we used the constant-gain beams in the numerical evaluation. Naturally, in practical networks the antenna beams are wider and likely irregular, with side lobes that are often neglected in the literature; we plan to take into account some more realistic beam models in our future work. Finally, we neglected the overhead needed for beamforming training and subsequent beam tracking, but it could be interesting to include it and analyze the impact of imperfect beam alignment on the communication performance, as well as the presence of obstacles in the communication paths.

APPENDIX A

Here we prove that STAs in group $n_{I,1}$ have the phase of their polar coordinates in the range $[\varphi_{\text{lim}}(d_i), 2\pi - \varphi_{\text{lim}}(d_i)]$, with φ_{lim} given in (26). Consider a possible interferer I at distance $d_i \in [0, R]$ from the AP and with angular phase $\varphi \in [0, \pi]$; this means that we are only focusing on the upper half of the circular area around the AP, being the scenario symmetric.

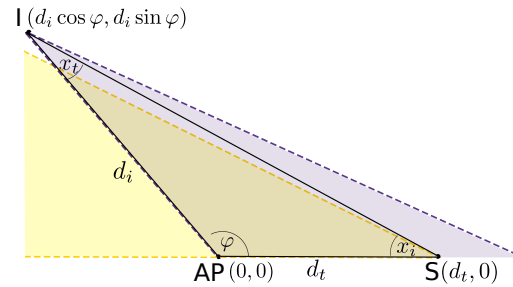


Figure 12: Target STA S and potential interferer I in the Cartesian plane. The blue area is the right half of the beam of I directed towards the AP in $(0, 0)$, with width $\theta_S/2$. Analogously, the yellow area is the upper half of the beam of S . The two STAs cannot hear each other, since the antenna gain of S in $(d_i \cos \varphi, d_i \sin \varphi)$ is zero; this means that $\varphi < \varphi_{\text{lim}}(d_i)$.

Consider the triangle whose vertices are the AP $(0, 0)$, the target STA S in $(d_t, 0)$ and I in $(d_i \cos \varphi, d_i \sin \varphi)$, as in Fig. 12. The two edges that form the AP vertex have length d_i and d_t , and the angle they form has width φ . Denote the other two angles as x_i and x_t , as in Fig. 12. We are interested in the angles φ such that S is in the beam of I , i.e., $x_i \leq \theta_S/2$, and I is in the beam of S , i.e., $x_t \leq \theta_S/2$ (the beams are symmetric with respect to the AP and have width θ_S). Moreover, the angles must satisfy the two following equations

$$x_i + x_t + \varphi = \pi, \quad \frac{d_i}{\sin x_i} = \frac{d_t}{\sin x_t}. \quad (33)$$

If $d_i \leq d_t$, then $x_i \geq x_t$, and thus the limit condition is obtained for $x_i = \theta_S/2$. Considering (33), we obtain that we are interested in all angles $\varphi \geq \varphi_{\text{lim}} = \pi - \theta_S/2 - \arcsin(d_i/d_t \sin \theta_S/2)$. Similarly, when $d_i > d_t$, the limit condition is obtained for $x_t = \theta_S/2$, yielding $\varphi_{\text{lim}} = \pi - \theta_S/2 - \arcsin(d_t/d_i \sin \theta_S/2)$. This proves Eq. (26). Taking into account also STAs in the lower half of the area around the AP, we finally obtain that the other STAs can overhear the messages sent by S if and only if their phase is in $[\varphi_{\text{lim}}(d_i), 2\pi - \varphi_{\text{lim}}(d_i)]$, with d_i being their distance from the AP.

APPENDIX B

Here we explain how to express (30) and (31) so as to compute them in closed form. We focus only on the first of the two integrals in (30), since analogous considerations can be made for the second one, and refer to it as $I_1 = \int_0^R \int_{\varphi_{\text{lim}}(r)}^{\varphi_{\text{AP}}} \partial \theta_r \partial r$. I_1 is zero if $\varphi_{\text{lim}}(r) > \varphi_{\text{AP}}$ for the considered $r \in [0, R]$ and position d_t of the target node (see (26)). In particular $I_1 = 0$ if

$$\arcsin\left(c_1 \sin \frac{\theta_S}{2}\right) < \pi - \frac{\theta_S}{2} - \varphi_{\text{AP}} \quad (34)$$

with $c_1 = r/d_t$ if $r \leq d_t$ and $c_1 = d_t/r$ otherwise (as per (26)). We recall that $0 \leq \theta_S \leq \pi$ and $0 \leq \varphi_{\text{AP}} \leq \theta_{\text{AP}} \leq \pi$ by assumption. Introducing $c_2 \triangleq \pi - \theta_S/2 - \varphi_{\text{AP}}$, it is $-\pi/2 \leq c_2 \leq \pi$. Note also that $0 \leq c_1 \sin \theta_S/2 \leq 1$, yielding $0 \leq \arcsin(c_1 \sin \theta_S/2) \leq \pi/2$.

- If $c_2 \in [\pi/2, \pi]$, then the conditions in (34) are certainly true, yielding $I_1 = 0$. This happens if $\varphi_{\text{AP}} < \pi/2 - \theta_S/2$, whatever the value of d_t .
- Otherwise $c_2 \in [-\pi/2, \pi/2]$. In this range the sine is monotonically increasing, and can be applied to both

terms in (34). This gives the condition $c_1 \sin \theta_S/2 < \sin(\pi - \theta_S/2 - \varphi_{AP})$, which can be expressed as $c_1 < \sin(\pi - \frac{\theta_S}{2} - \varphi_{AP}) / \sin \frac{\theta_S}{2} \triangleq c_3$. Thus, $I_1 = 0$ if $r < d_t c_3$ in the case $r \leq d_t$ and if $r > d_t/c_3$ in the case $r > d_t$. This happens only if $c_3 \leq 1$, i.e., $\phi_{AP} < \pi - \theta_S$.

Summing up, it is

$$I_1 = \left(\int_{\max(d_t c_3, 0)}^{d_t} \left(-c_2 + \arcsin\left(\frac{r}{d_t} \sin \frac{\theta_S}{2}\right) \right) r \partial r \right. \\ \left. + \int_{d_t}^{\min(\frac{d_t}{c_3}, R)} \left(-c_2 + \arcsin\left(\frac{d_t}{r} \sin \frac{\theta_S}{2}\right) \right) r \partial r \right) \mathbb{1}_{\varphi_{AP} \geq \pi - \theta_S} \quad (35)$$

with $\mathbb{1}_X$ being the indicator function, equal to 1 if condition X is true, and to 0 otherwise. The min and max operators in the integral limits ensure that the range $[0, R]$ is not exceeded. Eq. (35) can be solved in closed form: to this aim, it is necessary to evaluate the integration limits where there are the max and min operators. The same procedure can be used to compute the second integral I_2 in (30) using $\theta_{AP} - \varphi_{AP}$ rather than φ_{AP} . This expression of $\mathcal{R}_{R,C}(d_t, \varphi_{AP})$ can be used to compute its expectation as in (31). We can focus only on the first double integral (the one over ϕ_{AP}), since analogous considerations can be made on the second one (the one over $\theta_{AP} - \phi_{AP}$). Such first integral is made over I_1 and I_2 . We consider only the integral over I_1 and denote it as J_1 ; the rest of the terms in (31) can then be derived following the same approach. It is necessary to characterize d_t/c_3 and $d_t c_3$ based on d_t and φ_{AP} , so as to remove the min and max operators in the terms in (35). It is $d_t c_3 > 0$ if $\varphi_{AP} \leq \pi - c$, and $d_t/c_3 < R$ if $d_t \leq R c_3$. Rigorously from (35), it is $J_1 = 0$ if $\phi_{AP} < \pi - \theta_S$. This can be checked beforehand as it only depends on system parameters. It is then possible to evaluate J_1 in closed form and, repeating the same procedure for the other terms in (31), calculate $E[\mathcal{R}_{R,C}]$.

REFERENCES

- [1] "IEEE 802.11ad, amendment 3: Enhancements for very high throughput in the 60 GHz band," Dec. 2012.
- [2] S. Kutty and D. Sen, "Beamforming for millimeter wave communications: An inclusive survey," *IEEE Communications Surveys & Tutorials*, vol. 18, no. 2, pp. 949–973, Second Quarter 2016.
- [3] B. Satchidanandan, S. Yau, P. Kumar, A. Aziz, A. Ekbal, and N. Kundargi, "TrackMAC: An IEEE 802.11ad-compatible beam tracking-based MAC protocol for 5G millimeter-wave local area networks," in *International Conference on Communication Systems & Networks (COMSNETS)*. IEEE, Jan. 2018, pp. 185–182.
- [4] G. Bianchi, "Performance analysis of the IEEE 802.11 distributed coordination function," *IEEE Journal on Selected Areas in Communications*, vol. 18, no. 3, pp. 535–547, March 2000.
- [5] A. Akhtar and S. C. Ergen, "Directional MAC protocol for IEEE 802.11ad based wireless local area networks," *Ad Hoc Networks*, vol. 69, pp. 49–64, Feb. 2018.
- [6] T. Nitsche, C. Cordeiro, A. B. Flores, E. W. Knightly, E. Perahia, and J. C. Widmer, "IEEE 802.11ad: directional 60 GHz communication for multi-Gigabit-per-second Wi-Fi," *IEEE Comm. Magazine*, vol. 52, no. 12, pp. 132–141, Dec. 2014.
- [7] P. Chatzimisios, A. C. Boucouvalas, and V. Vitsas, "IEEE 802.11 packet delay—a finite retry limit analysis," in *IEEE Global Telecommunications Conference, (GLOBECOM'03)*, vol. 2. IEEE, Dec. 2003, pp. 950–954.
- [8] J. W. Robinson and T. S. Randhawa, "Saturation throughput analysis of IEEE 802.11e enhanced distributed coordination function," *IEEE Journal on Selected Areas in Communications*, vol. 22, no. 5, pp. 917–928, Aug. 2004.

- [9] F.-Y. Hung and I. Marsic, "Performance analysis of the IEEE 802.11 DCF in the presence of the hidden stations," *Computer Networks*, vol. 54, no. 15, pp. 2674–2687, Oct. 2010.
- [10] K. Chandra, R. V. Prasad, and I. Niemegeers, "Performance analysis of IEEE 802.11ad MAC protocol," *IEEE Communications Letters*, vol. 21, no. 7, pp. 1513–1516, July 2017.
- [11] C. Hemanth and T. Venkatesh, "Performance analysis of contention-based access periods and service periods of 802.11ad hybrid medium access control," *IET Networks*, vol. 3, no. 3, pp. 193–203, Sept. 2013.
- [12] M. N. Upama Rajan and A. V. Babu, "Saturation throughput analysis of IEEE 802.11ad wireless LAN in the contention based access period (CBAP)," in *IEEE Distributed Computing, VLSI, Electrical Circuits and Robotics*, 2016, pp. 41–46.
- [13] Q. Chen, J. Tang, D. T. C. Wong, X. Peng, and Y. Zhang, "Directional cooperative MAC protocol design and performance analysis for IEEE 802.11ad WLANs," *IEEE Tran. on Vehicular Technology*, vol. 62, no. 6, pp. 2667–2677, July 2013.
- [14] F. Babich and M. Comisso, "Throughput and delay analysis of 802.11-based wireless networks using smart and directional antennas," *IEEE Transactions on Communications*, vol. 57, no. 5, pp. 1413–1423, May 2009.
- [15] M. N. Upama Rajan and A. V. Babu, "Theoretical maximum throughput of IEEE 802.11ad millimeter wave wireless LAN in the contention based access period: With two level aggregation," in *International Conference on Wireless Communications, Signal Processing and Networking (WiSP-NET)*. IEEE, March 2017, pp. 2531–2536.
- [16] H. Shokri-Ghadikolaei, L. Gkatzikis, and C. Fischione, "Beam-searching and transmission scheduling in millimeter wave communications," in *IEEE International Conference on Communications (ICC)*. IEEE, June 2015, pp. 1292–1297.
- [17] P. Zhou, X. Fang, Y. Fang, Y. Long, R. He, and X. Han, "Enhanced random access and beam training for millimeter wave wireless local networks with high user density," *IEEE Transactions on Wireless Communications*, vol. 16, no. 12, pp. 7760–7773, Dec. 2017.
- [18] E. Khorov, A. Ivanov, A. Lyakhov, and V. Zankin, "Mathematical model for scheduling in IEEE 802.11ad networks," in *Wireless and Mobile Networking Conference (WMNC)*. IEEE, July 2016, pp. 153–160.
- [19] W. L. Stutzman and G. A. Thiele, *Antenna theory and design*. John Wiley & Sons, 2012.
- [20] P. Zhou, K. Cheng, X. Han, X. Fang, Y. Fang, R. He, Y. Long, and Y. Liu, "IEEE 802.11 ay-based mmWave WLANs: Design challenges and solutions," *IEEE Comm. Surveys & Tutorials*, vol. 20, no. 3, pp. 1654–1681, Third Quarter 2018.